Available online at www.ijournalse.org

Emerging Science Journal

(ISSN: 2610-9182)

Vol. 6, No. 5, October, 2022

Detection Sensitivity of a Modified EWMA Control Chart with a Time Series Model with Fractionality and Integration

Piyatida Phanthuna [1*], Yupaporn Areepong [2]

[1] *Faculty of Science and Technology, Rajamangala University of Technology Phra Nakhon, 10800, Thailand.*

[2] *Faculty of Applied Science, King Mongkut's University of Technology North Bangkok, 10800, Thailand.*

Abstract

Among the many statistical process control charts, the modified exponentially weighted moving average (EWMA) control chart has been designed to swiftly detect a small shift in a process parameter. Herein, we propose two explicit formulas for the average run length (ARL) for integrated moving average (IMA) and fractional integrated moving average (FIMA) models combined with the modified EWMA control chart for time series prediction. The application of the suggested control chart procedures depends on the residuals of the IMA and FIMA models. The performance of the control chart with both models is evaluated by using the ARL. Explicit formulas for the ARL for the two models with the modified EWMA statistic are derived and their precision is compared with the numerical integral equation method. The explicit formulas could accurately predict the true ARL while markedly decreasing the computational processing time compared to the numerical integration method. The capabilities of the IMA and FIMA models with the modified EWMA control chart were studied by varying g times the last term and exponential smoothing parameter λ, with the relative mean index being used to evaluate these situations. The results show that the modified EWMA control chart with either model performed better than the original EWMA control chart. Furthermore, the modified EWMA control chart with either model was highly efficient when g increased and λ was small. Two applications involving energy commodity prices are used to illustrate the efficacies of the proposed approaches, the results of which were in accordance with the experimental study.

Keywords:

Explicit Formula;

Average Run Length;

Fractionally Integrated Moving Average;

Modified Exponentially Weighted Moving Average.

Article History:

Received:	20	April	2022
Revised:	27	June	2022
Accepted:	24	July	2022
Available online:	16	August	2022

1- Introduction

Control charts are key statistical process control tools used to monitor processes and verify product quality. In 1931, Shewhart [1] first proposed a control chart capable of detecting large changes in process parameters. Later, the cumulative sum (CUSUM) [2] and exponentially weighted moving average (EWMA) [3] monitoring charts were developed to detect small-to-moderate shifts in process parameters. The EWMA control chart is susceptible to small changes in process parameters and can be used to estimate observations in the next time period. Since then, the EWMA scheme has been updated to enhance its detection capability. Patel and Divecha (2011) [4] improved the EWMA statistic by expanding a different term based on previous observations and called it the modified EWMA control chart. After that, Khan et al. [5] developed a better approach for adjusting g multiplied by the last term of the modified EWMA statistic, thereby enabling it to quickly detect parameter changes in auto-correlated data series.

Autocorrelation in time series has been studied over a long period of time, and time series models have been used for forecasting in various situations, such as the COVID-19 pandemic [6], stock trends [7], and the weather [8]. Depending

* **CONTACT**: piyatida.r@rmutp.ac.th

DOI: http://dx.doi.org/10.28991/ESJ-2022-06-05-015

on the data trend, they are classified as autoregressive (AR) [9], moving average (MA) [10], autoregressive moving average (ARMA) [11], autoregressive integrated moving average (ARIMA) [12], and autoregressive fractional integrated moving average (ARFIMA) [13]. Moreover, integrated moving average (IMA) [14] and fractionally integrated moving average (FIMA) [15] models are special cases of ARIMA and ARFIMA processes, respectively. In some situations, IMA and FIMA models can be used to predict observations appropriately. An IMA model is a MA model added to the level of differencing d times, where d is an integer, while in the FIMA model, d is the fractional differencing parameter. IMA and FIMA models have been applied in various areas, such as industry [16], engineering [17], transportation [18], and biomedical science [19]. Most modeling of time series involves white noise [20], which is an uncorrelated stationary time series or random process following a normal distribution. In reality, it is frequently found that the residuals are exponentially distributed (i.e., exponential white noise).

The average run length (ARL) [21] is a statistical measure used extensively to test the performance of a control chart. It is the average number of observations needed until a signal occurs. Common techniques to estimate the ARL are Monte Carlo simulation [22, 23] and the numerical integral equation (NIE) [24, 25]. On the other hand, the exact ARL can be computed by using an explicit formula, albeit that it is not easy to define. However, the advantage is that they can be processed immediately and produce an accurate value. In this paper, explicit formulas for the ARL on the modified EWMA control charts with IMA and FIMA models and exponential white noise are proposed.

This article is organized as follows. Previous studies on explicit formulas for the ARL on control charts are reviewed in Section 2. The modified EWMA control chart and derivations of the explicit formulas and the NIE method for the ARL for the IMA and FIMA models with the modified EWMA control chart are introduced in Section 3. The research process is provided in Section 4. A comparison of the ARL solutions using the two techniques experimentally and with real data along with a performance comparison on the original and modified EWMA control charts for various situations are presented in Section 5. Finally, conclusions are given in Section 6.

2- Literature Review

Many researchers have proposed explicit formulas for the ARL on control charts with time series models. Petcharat et al. [26] presented explicit formulas for the ARL of random observations from a MA process with exponential white noise running on a CUSUM control chart; they compared the computational times of the explicit formulas and the NIE method and found that using the former was much faster. Sunthornwat et al. [27] proposed explicit formulas for the analytical ARL on an EWMA control chart with a long-memory ARFIMA model by using a solution for the integral equation and compared them with the NIE method; once again, the computational time for the former was much lower. Sunthornwat and Areepong [28] derived explicit formulas for the ARL for seasonal and non-seasonal MA processes with exogenous variables running on a CUSUM control chart and found their optimal parameters. When comparing the solution for a CUSUM control chart with that for an EWMA control chart, the former detected small process shifts better but moderate-to-large process shifts worse than the latter.

Phanthuna et al. [29] introduced process shift detection for the modified EWMA control chart with an AR(1) process and exponential white noise. Explicit formulas for the ARL were derived and checked with the NIE method in terms of accuracy and computational time. Although both produced ARLs similar to the exact ARL, the explicit formulas method was much faster than the NIE method in obtaining an accurate value. Moreover, the authors reported an efficiency comparison of the CUSUM, EWMA, and modified EWMA control charts; their proposed control chart provided the best performance for small-to-intermediate shifts in the process parameter. Later, Phanthuna et al. [30] improved the explicit formulas for computing ARL solutions for the modified EWMA scheme in that they could be used for any order p of an AR(p) model, where p is a positive integer. Supharakonsakun et al. [31] studied a detection procedure for the EWMA and modified EWMA control charts with an ARMA(1,1) process and exponential white noise. Explicit formulas for the exact ARL were provided and their accuracy was compared with the NIE method. Supharakonsakun et al. [32] suggested explicit formulas for the ARL with observations from a MA model on the modified EWMA control chart and compared their capability with the same process on the standard EWMA scheme for monitoring PM2.5 and carbon monoxide air pollution data; their results show that the modified EWMA control chart was much better at detecting shifts in the process parameter than the standard EWMA control chart. Supharakonsakun [33] designed the modified EWMA control chart for a seasonal MA model and evaluated its efficacy by using the ARL calculated via explicit formulas and the NIE method. The efficiencies of the method for the EWMA, CUSUM, and modified EWMA control charts for a seasonal MA process with exponential white noise support the superiority of the latter.

3- Control Chart for Time Series Models and Solving the ARL

3-1- The Modified EWMA Control Chart

The modified EWMA control chart can quickly detect a small shift in the process mean. In the EWMA statistic, the term $g(X_t - X_{t-1})$ from the modified EWMA control chart has been assigned to $g = 0$, and thus the modified EWMA statistic can be defined as:

$$Y_t = (1-\lambda)Y_{t-1} + \lambda X_t + g(X_t - X_{t-1}), \quad (1)$$

where λ is an exponential smoothing parameter where $0 < \lambda < 1$, X_t is the data sequence at $t = 1, 2, 3,...$ with mean μ and variance σ^2, and g is a suitable constant. The initial values of sequences Y_t and X_t ($t = 0$) are determined for μ and the asymptotic variance of Y_t as $(\lambda + 2\lambda g + 2g^2)\sigma^2/(2-\lambda)$. Thus, the bounds of the control limits of the modified EWMA control chart can be constructed for μ, σ, and suitable control width limit C as follows:

$$\mu \pm C\sigma\sqrt{\frac{\lambda+2\lambda g+2g^2}{2-\lambda}}$$

3-2- The IMA-Modified EWMA Control Chart

For time series, the ARIMA (p, d, q) model, where p is the order of the autoregressive process, d is the order of differencing, and q is the order of the MA process, is widely applied to real data from many fields. When there is no autoregression in the time series, the IMA model is equivalent to the ARIMA (0, d, q) model. The IMA (d, q) model, denoted as M_t, can be defined by using backward shift operator B as follows:

$$(1-B)^d M_t = \theta_0 + (1-\theta_1 B - \theta_2 B^2 - ... - \theta_q B^q)\varepsilon_t, \quad (2)$$

where, $(1-B)^d = \sum_{k=0}^{d} \binom{d}{k} (-B)^k$ is defined by using the Binomial Theorem [34]. Therefore, the IMA model can be rewritten as:

$$M_t = \theta_0 + (\varepsilon_t - \theta_1\varepsilon_{t-1} - \theta_2\varepsilon_{t-2} - ... - \theta_q\varepsilon_{t-q}) + \left(dM_{t-1} - \frac{d(d-1)}{2!}M_{t-2} + \frac{d(d-1)(d-2)}{3!}M_{t-3} - ... + (-1)^{d+1}M_{t-d} \right), \quad (3)$$

where, θ_0 is the process average, θ_i ($i = 1,2,\ldots,q$) are the coefficients of the IMA model ($-1 < \theta_i < 1$) and ε_{t-i} is exponential white noise at time t.

3-2-1- The Explicit Formula for the ARL on the Modified EWMA Control Chart with the IMA Model

The ARL, which is the average number of observations before an alarm occurs, is a commonly used measure for the sensitivity of a control chart. In this section, the explicit formula for the ARL on the modified EWMA control chart with the IMA model is solved. From Equations 1 and 3, the modified EWMA statistic for the IMA model can be derived as:

$$\begin{aligned} Y_t = {} & (1-\lambda)Y_{t-1} - gM_{t-1} + (\lambda+g)\varepsilon_t + (\lambda+g)(\theta_0 - \theta_1\varepsilon_{t-1} - \theta_2\varepsilon_{t-2} - ... - \theta_q\varepsilon_{t-q}) \\ & + (\lambda+g)\left(dM_{t-1} - \frac{d(d-1)}{2!}M_{t-2} + \frac{d(d-1)(d-2)}{3!}M_{t-3} - ... + (-1)^{d+1}M_{t-d} \right). \end{aligned}$$

The lower and upper bounds of the control limits are l and h, respectively. For the in-control process, the interval of Y_t can be written as:

$$l < \left[\begin{array}{l} (1-\lambda)Y_t - gM_{t-1} + (\lambda+g)\varepsilon_t + (\lambda+g)(\theta_0 - \theta_1\varepsilon_{t-1} - \theta_2\varepsilon_{t-2} - ... - \theta_q\varepsilon_{t-q}) \\ +(\lambda+g)\left(dM_{t-1} - \frac{d(d-1)}{2!}M_{t-2} + \frac{d(d-1)(d-2)}{3!}M_{t-3} - ... + (-1)^{d+1}M_{t-d} \right) \end{array} \right] < h.$$

This interval can be rearranged on variable ε_t to provide:

$$\left[\begin{array}{l} \dfrac{l - (1-\lambda)Y_t + gM_{t-1}}{(\lambda+g)} \\ -(\theta_0 - \theta_1\varepsilon_{t-1} - \theta_2\varepsilon_{t-2} - ... - \theta_q\varepsilon_{t-q}) \\ -\left(\begin{array}{l} dM_{t-1} - \dfrac{d(d-1)}{2!}M_{t-2} \\ +\dfrac{d(d-1)(d-2)}{3!}M_{t-3} - ... + (-1)^{d+1}M_{t-d} \end{array} \right) \end{array} \right] < \varepsilon_t < \left[\begin{array}{l} \dfrac{h - (1-\lambda)Y_t + gM_{t-1}}{(\lambda+g)} \\ -(\theta_0 - \theta_1\varepsilon_{t-1} - \theta_2\varepsilon_{t-2} - ... - \theta_q\varepsilon_{t-q}) \\ -\left(\begin{array}{l} dM_{t-1} - \dfrac{d(d-1)}{2!}M_{t-2} \\ +\dfrac{d(d-1)(d-2)}{3!}M_{t-3} - ... + (-1)^{d+1}M_{t-d} \end{array} \right) \end{array} \right]$$

$$L < \varepsilon_t < H.$$

The integral equation for the ARL on the modified EWMA control chart with an IMA (d, q) process and initial value $Y_0 = u$ is derived by using the Fredholm integral equation [35] as follows:

$$T_{ARL}(u) = 1 + \int_{L}^{H} T_{ARL}\begin{pmatrix} (\lambda+g)y + (1-\lambda)u - gM_{t-1} + (\lambda+g)\left(\theta_0 - \theta_1\varepsilon_{t-1} - \theta_2\varepsilon_{t-2} - \ldots - \theta_q\varepsilon_{t-q}\right) \\ +(\lambda+g)\left(dM_{t-1} - \frac{d(d-1)}{2!}M_{t-2} + \frac{d(d-1)(d-2)}{3!}M_{t-3} - \ldots + (-1)^{d+1}M_{t-d}\right) \end{pmatrix} \cdot f(y)\,dy.$$

By solving the integral equation, the integral variable can be adjusted by setting $x = (\lambda+g)y + (1-\lambda)u - gM_{t-1} + (\lambda+g)(\theta_0 - \theta_1\varepsilon_{t-1} - \theta_2\varepsilon_{t-2} - \cdots - \theta_q\varepsilon_{t-q} + (\lambda+g)(dM_{t-1} - \frac{d(d-1)}{2!}M_{t-2} + \frac{d(d-1)(d-2)}{3!}M_{t-3} - \cdots + (-1)^{d+1}M_{t-d}$. Thus, T_{ARL} can be reworked as:

$$T_{ARL}(u) = 1 + \frac{1}{\lambda+g}\int_{l}^{h} T_{ARL}(x)\, f\begin{pmatrix} \frac{x-(1-\lambda)u+gM_{t-1}}{(\lambda+g)} \\ -\left(\theta_0 - \theta_1\varepsilon_{t-1} - \theta_2\varepsilon_{t-2} - \ldots - \theta_q\varepsilon_{t-q}\right) \\ -\left(dM_{t-1} - \frac{d(d-1)}{2!}M_{t-2} + \frac{d(d-1)(d-2)}{3!}M_{t-3} - \ldots + (-1)^{d+1}M_{t-d}\right) \end{pmatrix} dx. \quad (4)$$

Since the function of ε_t is exponential, then $T_{ARL}(u)$ can be rewritten as:

$$T_{ARL}(u) = 1 + \frac{e^{\frac{(1-\lambda)u}{\beta(\lambda+g)}} \cdot e^{\frac{-gM_{t-1}}{\beta(\lambda+g)}} \cdot e^{\frac{\theta_0 - \theta_1\varepsilon_{t-1} - \theta_2\varepsilon_{t-2} - \ldots - \theta_q\varepsilon_{t-q}}{\beta}} \cdot e^{\frac{dM_{t-1} - \frac{d(d-1)}{2!}M_{t-2} + \frac{d(d-1)(d-2)}{3!}M_{t-3} - \ldots + (-1)^{d+1}M_{t-d}}{\beta}}}{\beta(\lambda+g)} \int_{l}^{h} e^{\frac{-x}{\beta(\lambda+g)}} \cdot T_{ARL}(x)\,dx. \quad (5)$$

After checking the uniqueness of the ARL solution by using Banach's fixed point theorem [36], the explicit formula for the ARL of the IMA model on the modified EWMA control chart is derived by setting $P = \int_{l}^{h} e^{\frac{-x}{\beta(\lambda+g)}} \cdot T_{ARL}(x)dx$ and substituting P in Equation 5 as follows:

$$T_{ARL}(u) = 1 + \frac{e^{\frac{(1-\lambda)u}{\beta(\lambda+g)}} \cdot e^{\frac{-gM_{t-1}}{\beta(\lambda+g)}} \cdot e^{\frac{\theta_0 - \theta_1\varepsilon_{t-1} - \theta_2\varepsilon_{t-2} - \ldots - \theta_q\varepsilon_{t-q}}{\beta}} \cdot e^{\frac{dM_{t-1} - \frac{d(d-1)}{2!}M_{t-2} + \frac{d(d-1)(d-2)}{3!}M_{t-3} - \ldots + (-1)^{d+1}M_{t-d}}{\beta}}}{\beta(\lambda+g)} \cdot P. \quad (7)$$

Afterward, integral equation P can be obtained as:

$$P = \int_{l}^{h} e^{\frac{-x}{\beta(\lambda+g)}} \left(1 + \frac{e^{\frac{(1-\lambda)x}{\beta(\lambda+g)}} \cdot e^{\frac{-gM_{t-1}}{\beta(\lambda+g)}} \cdot e^{\frac{\theta_0 - \theta_1\varepsilon_{t-1} - \theta_2\varepsilon_{t-2} - \ldots - \theta_q\varepsilon_{t-q}}{\beta}} \cdot e^{\frac{dM_{t-1} - \frac{d(d-1)}{2!}M_{t-2} + \frac{d(d-1)(d-2)}{3!}M_{t-3} - \ldots + (-1)^{d+1}M_{t-d}}{\beta}}}{\beta(\lambda+g)} \cdot P \right) dx$$

$$P = -\beta(\lambda+g)\left[e^{\frac{-h}{\beta(\lambda+g)}} - e^{\frac{-l}{\beta(\lambda+g)}} \right]$$

$$- \frac{e^{\frac{-gM_{t-1}}{\beta(\lambda+g)}} \cdot e^{\frac{\theta_0 - \theta_1\varepsilon_{t-1} - \theta_2\varepsilon_{t-2} - \ldots - \theta_q\varepsilon_{t-q}}{\beta}} \cdot e^{\frac{dM_{t-1} - \frac{d(d-1)}{2!}M_{t-2} + \frac{d(d-1)(d-2)}{3!}M_{t-3} - \ldots + (-1)^{d+1}M_{t-d}}{\beta}}}{\lambda} \cdot P \left[e^{\frac{-h\lambda}{\beta(\lambda+g)}} - e^{\frac{-l\lambda}{\beta(\lambda+g)}} \right]$$

$$P = \frac{-\beta(\lambda+g)\left[e^{\frac{-h}{\beta(\lambda+g)}} - e^{\frac{-l}{\beta(\lambda+g)}} \right]}{1 + \frac{e^{\frac{-gM_{t-1}}{\beta(\lambda+g)}} \cdot e^{\frac{\theta_0 - \theta_1\varepsilon_{t-1} - \theta_2\varepsilon_{t-2} - \ldots - \theta_q\varepsilon_{t-q}}{\beta}} \cdot e^{\frac{dM_{t-1} - \frac{d(d-1)}{2!}M_{t-2} + \frac{d(d-1)(d-2)}{3!}M_{t-3} - \ldots + (-1)^{d+1}M_{t-d}}{\beta}}}{\lambda} \left[e^{\frac{-h\lambda}{\beta(\lambda+g)}} - e^{\frac{-l\lambda}{\beta(\lambda+g)}} \right]}.$$

By using the solution for P to solve the integral equation for $T_{ARL}(u)$ in Equation 6, we attain the explicit formula for the ARL on the modified EWMA control chart with the IMA model as:

$$T_{ARL}(u)=1-\frac{e^{\frac{(1-\lambda)u}{\beta(\lambda+g)}}\cdot e^{\frac{-gM_{t-1}}{\beta(\lambda+g)}}\cdot e^{\frac{\theta_0-\theta_1\varepsilon_{t-1}-\theta_2\varepsilon_{t-2}-\ldots-\theta_q\varepsilon_{t-q}}{\beta}}\cdot e^{\frac{dM_{t-1}-\frac{d(d-1)}{2!}M_{t-2}+\frac{d(d-1)(d-2)}{3!}M_{t-3}-\ldots+(-1)^{d+1}M_{t-d}}{\beta}}\left[e^{\frac{-h}{\beta(\lambda+g)}}-e^{\frac{-l}{\beta(\lambda+g)}}\right]}{1+\frac{e^{\frac{-gM_{t-1}}{\beta(\lambda+g)}}\cdot e^{\frac{\theta_0-\theta_1\varepsilon_{t-1}-\theta_2\varepsilon_{t-2}-\ldots-\theta_q\varepsilon_{t-q}}{\beta}}\cdot e^{\frac{dM_{t-1}-\frac{d(d-1)}{2!}M_{t-2}+\frac{d(d-1)(d-2)}{3!}M_{t-3}-\ldots+(-1)^{d+1}M_{t-d}}{\beta}}\left[e^{\frac{-h\lambda}{\beta(\lambda+g)}}-e^{\frac{-l\lambda}{\beta(\lambda+g)}}\right]}{\lambda}}$$

$$T_{ARL}(u)=1-\frac{\lambda\cdot e^{\frac{(1-\lambda)u}{\beta(\lambda+g)}}\left[e^{\frac{-h}{\beta(\lambda+g)}}-e^{\frac{-l}{\beta(\lambda+g)}}\right]}{\lambda\cdot e^{\frac{gM_{t-1}}{\beta(\lambda+g)}}\cdot e^{-\frac{\theta_0-\theta_1\varepsilon_{t-1}-\theta_2\varepsilon_{t-2}-\ldots-\theta_q\varepsilon_{t-q}}{\beta}}\cdot e^{-\frac{dM_{t-1}-\frac{d(d-1)}{2!}M_{t-2}+\frac{d(d-1)(d-2)}{3!}M_{t-3}-\ldots+(-1)^{d+1}M_{t-d}}{\beta}}+e^{\frac{-h\lambda}{\beta(\lambda+g)}}-e^{\frac{-l\lambda}{\beta(\lambda+g)}}}. \quad (7)$$

3-2-2- The NIE Method for the ARL on the Modified EWMA Control Chart with the IMA Model

The NIE method is a technique for accurately approximating the ARL that can be used to determine the efficacy of explicit formula derivations. In this section, $NT_{ARL}(u)$ is defined by using the NIE method with Simpson's quadrature rule [37] to estimate the ARL on the modified EWMA control chart with the IMA model and exponential white noise. The integral equation in Equation 4 is solved by using a $2m+1$ linear equation system on interval $[l, h]$ with length $2m$. After that, the weight of each point is determined as follows: the start and end points ($w_j = v_j/3$) and the even and odd points within the interval ($w_j = 4v_j/3$ and $w_j = 2v_j/3$, respectively) such that $v_j = (h - l)/2m$; $j = 0, 1, 2, \ldots, 2m$. and $x_{j+1} = jw_{j+1} + l$. Finally, the NIE method provides:

$$NT_{ARL}(u)\approx 1+\frac{1}{\lambda+g}\sum_{j=1}^{2m+1}w_j\cdot T_{ARL}(x_j)\cdot f\left(\begin{array}{l}\frac{x_j-(1-\lambda)u+gM_{t-1}}{(\lambda+g)}\\ -\left(\theta_0-\theta_1\varepsilon_{t-1}-\theta_2\varepsilon_{t-2}-\ldots-\theta_q\varepsilon_{t-q}\right)\\ -\left(dM_{t-1}-\frac{d(d-1)}{2!}M_{t-2}+\frac{d(d-1)(d-2)}{3!}M_{t-3}-\ldots+(-1)^{d+1}M_{t-d}\right)\end{array}\right). \quad (8)$$

3-3- The FIMA-Modified EWMA Control Chart

For some cases, parameter d of the IMA model must be expressed as a fraction (where $-\frac{1}{2}\le d\le\frac{1}{2}$) rather than an integer, thereby providing the fractional integrated MA (FIMA) model. For the pattern of backward shift operator B, the FIMA (a/b, q) model or F_t is defined as:

$$(1-B)^{a/b}F_t=\theta_0+\left(1-\theta_1B-\theta_2B^2-\ldots-\theta_qB^q\right)\varepsilon_t, \quad (9)$$

where, a and b are constants ($a < b$). By applying the generalized Newton binomial theorem [38],$(1-B)^{a/b}=\sum_{k=0}^{\infty}\binom{a/b}{k}(-B)^k$, the FIMA model can be solved as:

$$F_t=\theta_0+\left(\varepsilon_t-\theta_1\varepsilon_{t-1}-\theta_2\varepsilon_{t-2}-\ldots-\theta_q\varepsilon_{t-q}\right)+\left(\frac{a}{b}F_{t-1}+\frac{\frac{a}{b}(1-\frac{a}{b})}{2!}F_{t-2}+\frac{\frac{a}{b}(1-\frac{a}{b})(2-\frac{a}{b})}{3!}F_{t-3}+\ldots\right), \quad (10)$$

where, θ_0 is the process average, θ_i ($i = 1,2,\ldots,q$) are the coefficients of the FIMA model ($-1< \theta_i <1$) and ε_{t-i} is exponential white noise at time t.

3-3-1- The Explicit Formula for the ARL on the Modified EWMA Control Chart with the FIMA Model

For the FIMA model, the modified EWMA statistic created by combining Equations 1 and 10 can be rewritten as:

$$Y_t = (1-\lambda)Y_{t-1} - gF_{t-1} + (\lambda+g)\varepsilon_t + (\lambda+g)\left(\theta_0 - \theta_1\varepsilon_{t-1} - \theta_2\varepsilon_{t-2} - \ldots - \theta_q\varepsilon_{t-q}\right) + (\lambda+g)\left(\frac{a}{b}F_{t-1} + \frac{\frac{a}{b}(1-\frac{a}{b})}{2!}F_{t-2} + \frac{\frac{a}{b}(1-\frac{a}{b})(2-\frac{a}{b})}{3!}F_{t-3} + \ldots\right).$$

The interval for modified EWMA statistic Y_t is defined under the lower (r) and upper (s) bounds before an observation that is out-of-control occurs as follows:

$$r < \left[\begin{array}{l}(1-\lambda)Y_{t-1} - gF_{t-1} + (\lambda+g)\varepsilon_t + (\lambda+g)\left(\theta_0 - \theta_1\varepsilon_{t-1} - \theta_2\varepsilon_{t-2} - \ldots - \theta_q\varepsilon_{t-q}\right) \\ +(\lambda+g)\left(\frac{a}{b}F_{t-1} + \frac{\frac{a}{b}(1-\frac{a}{b})}{2!}F_{t-2} + \frac{\frac{a}{b}(1-\frac{a}{b})(2-\frac{a}{b})}{3!}F_{t-3} + \ldots\right)\end{array}\right] < s.$$

The interval of ε_t can be derived as:

$$\left[\begin{array}{l}\frac{r-(1-\lambda)Y_t + gF_{t-1}}{(\lambda+g)} \\ -\left(\theta_0 - \theta_1\varepsilon_{t-1} - \theta_2\varepsilon_{t-2} - \ldots - \theta_q\varepsilon_{t-q}\right) \\ -\left(\frac{a}{b}F_{t-1} + \frac{\frac{a}{b}(1-\frac{a}{b})}{2!}F_{t-2} + \frac{\frac{a}{b}(1-\frac{a}{b})(2-\frac{a}{b})}{3!}F_{t-3} + \ldots\right)\end{array}\right] < \varepsilon_t < \left[\begin{array}{l}\frac{s-(1-\lambda)Y_t + gF_{t-1}}{(\lambda+g)} \\ -\left(\theta_0 - \theta_1\varepsilon_{t-1} - \theta_2\varepsilon_{t-2} - \ldots - \theta_q\varepsilon_{t-q}\right) \\ -\left(\frac{a}{b}F_{t-1} + \frac{\frac{a}{b}(1-\frac{a}{b})}{2!}F_{t-2} + \frac{\frac{a}{b}(1-\frac{a}{b})(2-\frac{a}{b})}{3!}F_{t-3} + \ldots\right)\end{array}\right]$$

$$R < \varepsilon_t < S.$$

The integral equation of the second kind is used to find the explicit formula for the ARL on a modified EWMA control chart with the FIMA model given initial value $Y_0 = u$ as follows:

$$E_{ARL}(u) = 1 + \int_S^R E_{ARL}\left(\begin{array}{l}(\lambda+g)y + (1-\lambda)u - gF_{t-1} + (\lambda+g)\left(\theta_0 - \theta_1\varepsilon_{t-1} - \theta_2\varepsilon_{t-2} - \ldots - \theta_q\varepsilon_{t-q}\right) \\ +(\lambda+g)\left(\frac{a}{b}F_{t-1} + \frac{\frac{a}{b}(1-\frac{a}{b})}{2!}F_{t-2} + \frac{\frac{a}{b}(1-\frac{a}{b})(2-\frac{a}{b})}{3!}F_{t-3} + \ldots\right)\end{array}\right) \cdot f(y)\,dy.$$

For solving the integral equation for $E_{ARL}(u)$, $x = (\lambda+g)y + (1-\lambda)u - gF_{t-1} + (\lambda+g)(\theta_0 - \theta_1\varepsilon_{t-1} - \theta_2\varepsilon_{t-2} - \cdots - \theta_q\varepsilon_{t-q} + (\lambda+g)(\frac{a}{b}F_{t-1} + \frac{\frac{a}{b}(1-\frac{a}{b})}{2!}F_{t-2} + \frac{\frac{a}{b}(1-\frac{a}{b})(2-\frac{a}{b})}{3!}F_{t-3} + \cdots$ is applied as follows:

$$E_{ARL}(u) = 1 + \frac{1}{\lambda+g}\int_r^s E_{ARL}(x)\, f\left(\begin{array}{l}\frac{x-(1-\lambda)u + gF_{t-1}}{(\lambda+g)} \\ -\left(\theta_0 - \theta_1\varepsilon_{t-1} - \theta_2\varepsilon_{t-2} - \ldots - \theta_q\varepsilon_{t-q}\right) \\ -\left(\frac{a}{b}F_{t-1} + \frac{\frac{a}{b}(1-\frac{a}{b})}{2!}F_{t-2} + \frac{\frac{a}{b}(1-\frac{a}{b})(2-\frac{a}{b})}{3!}F_{t-3} + \ldots\right)\end{array}\right) dx. \quad (11)$$

Moreover, $E_{ARL}(u)$ can be rearranged by using the exponential distribution of the error term ε_t as:

$$E_{ARL}(u) = 1 + \frac{e^{\frac{(1-\lambda)u}{\beta(\lambda+g)}} \cdot e^{\frac{-gF_{t-1}}{\beta(\lambda+g)}} \cdot e^{\frac{\theta_0 - \theta_1\varepsilon_{t-1} - \theta_2\varepsilon_{t-2} - \ldots - \theta_q\varepsilon_{t-q}}{\beta}} \cdot e^{\frac{\frac{a}{b}F_{t-1} + \frac{\frac{a}{b}(1-\frac{a}{b})}{2!}F_{t-2} + \frac{\frac{a}{b}(1-\frac{a}{b})(2-\frac{a}{b})}{3!}F_{t-3} + \ldots}{\beta}}}{\beta(\lambda+g)} \int_r^s e^{\frac{-x}{\beta(\lambda+g)}} \cdot E_{ARL}(x)\,dx. \quad (12)$$

The uniqueness of the ARL formula was verified by using Banach's fixed point theorem. Equation 12 is solved by determining $Q = \int_r^s e^{\frac{-x}{\beta(\lambda+g)}} \cdot E_{ARL}(x)dx$. Subsequently, $E_{ARL}(u)$ can be rewritten as:

$$E_{ARL}(u) = 1 + \frac{e^{\frac{(1-\lambda)u}{\beta(\lambda+g)}} \cdot e^{\frac{-gF_{t-1}}{\beta(\lambda+g)}} \cdot e^{\frac{\theta_0 - \theta_1\varepsilon_{t-1} - \theta_2\varepsilon_{t-2} - \ldots - \theta_q\varepsilon_{t-q}}{\beta}} \cdot e^{\frac{\frac{a}{b}F_{t-1} + \frac{\frac{a}{b}(1-\frac{a}{b})}{2!}F_{t-2} + \frac{\frac{a}{b}(1-\frac{a}{b})(2-\frac{a}{b})}{3!}F_{t-3} + \ldots}{\beta}}}{\beta(\lambda+g)} \cdot Q. \tag{13}$$

Since $Q = \int_r^s e^{\frac{-x}{\beta(\lambda+g)}} \cdot E_{ARL}(x)dx$, then $E_{ARL}(u)$ in Equation 13 is put into Q as follows:

$$Q = \int_r^s e^{\frac{-x}{\beta(\lambda+g)}} \left(1 + \frac{e^{\frac{(1-\lambda)x}{\beta(\lambda+g)}} \cdot e^{\frac{-gF_{t-1}}{\beta(\lambda+g)}} \cdot e^{\frac{\theta_0 - \theta_1\varepsilon_{t-1} - \theta_2\varepsilon_{t-2} - \ldots - \theta_q\varepsilon_{t-q}}{\beta}} \cdot e^{\frac{\frac{a}{b}F_{t-1} + \frac{\frac{a}{b}(1-\frac{a}{b})}{2!}F_{t-2} + \frac{\frac{a}{b}(1-\frac{a}{b})(2-\frac{a}{b})}{3!}F_{t-3} + \ldots}{\beta}}}{\beta(\lambda+g)} \cdot Q \right) dx$$

$$Q = -\beta(\lambda+g)\left[e^{\frac{-s}{\beta(\lambda+g)}} - e^{\frac{-r}{\beta(\lambda+g)}} \right] - \frac{e^{\frac{-gF_{t-1}}{\beta(\lambda+g)}} \cdot e^{\frac{\theta_0 - \theta_1\varepsilon_{t-1} - \theta_2\varepsilon_{t-2} - \ldots - \theta_q\varepsilon_{t-q}}{\beta}} \cdot e^{\frac{\frac{a}{b}F_{t-1} + \frac{\frac{a}{b}(1-\frac{a}{b})}{2!}F_{t-2} + \frac{\frac{a}{b}(1-\frac{a}{b})(2-\frac{a}{b})}{3!}F_{t-3} + \ldots}{\beta}}}{\lambda} \cdot Q \left[e^{\frac{-s\lambda}{\beta(\lambda+g)}} - e^{\frac{-r\lambda}{\beta(\lambda+g)}} \right]$$

$$Q = \frac{-\beta(\lambda+g)\left[e^{\frac{-s}{\beta(\lambda+g)}} - e^{\frac{-r}{\beta(\lambda+g)}} \right]}{1 + \frac{e^{\frac{-gF_{t-1}}{\beta(\lambda+g)}} \cdot e^{\frac{\theta_0 - \theta_1\varepsilon_{t-1} - \theta_2\varepsilon_{t-2} - \ldots - \theta_q\varepsilon_{t-q}}{\beta}} \cdot e^{\frac{\frac{a}{b}F_{t-1} + \frac{\frac{a}{b}(1-\frac{a}{b})}{2!}F_{t-2} + \frac{\frac{a}{b}(1-\frac{a}{b})(2-\frac{a}{b})}{3!}F_{t-3} + \ldots}{\beta}}}{\lambda} \left[e^{\frac{-s\lambda}{\beta(\lambda+g)}} - e^{\frac{-r\lambda}{\beta(\lambda+g)}} \right]}.$$

After Q has been obtained and substituted into 13, then the explicit formula for ARL on the modified EWMA control chart with the FIMA (a/b, q) model called $E_{ARL}(u)$ can be defined as:

$$E_{ARL}(u) = 1 - \frac{\lambda \cdot e^{\frac{(1-\lambda)u}{\beta(\lambda+g)}} \left[e^{\frac{-s}{\beta(\lambda+g)}} - e^{\frac{-r}{\beta(\lambda+g)}} \right]}{\lambda \cdot e^{\frac{gF_{t-1}}{\beta(\lambda+g)}} \cdot e^{-\frac{\theta_0 - \theta_1\varepsilon_{t-1} - \theta_2\varepsilon_{t-2} - \ldots - \theta_q\varepsilon_{t-q}}{\beta}} \cdot e^{-\frac{\frac{a}{b}F_{t-1} + \frac{\frac{a}{b}(1-\frac{a}{b})}{2!}F_{t-2} + \frac{\frac{a}{b}(1-\frac{a}{b})(2-\frac{a}{b})}{3!}F_{t-3} + \ldots}{\beta}} + e^{\frac{-s\lambda}{\beta(\lambda+g)}} - e^{\frac{-r\lambda}{\beta(\lambda+g)}}}. \tag{14}$$

3-3-2- The NIE Method for the ARL on the Modified EWMA Control Chart with the FIMA Model

$NE_{ARL}(u)$ is the NIE technique with the Simpson's quadrature rule to approximate the ARL on the modified EWMA control chart with the FIMA model and exponential white noise. Similar to Equation 11, the $2m$ +1 linear equation system is derived for the integral equation of interval [r, s]. If the distance of this interval is $2m$, then $x_{j+1} = jw_{j+1} + l$; j = 0, 1, 2, …, $2m$ are various points within it, where the weight of the start and end points is $w_j = v_j/3$ and the even and odd points within the interval are $w_j = 4v_j/3$ and $w_j = 2v_j/3$, respectively, and $v_j = (s - r)/2m$. Finally, $NE_{ARL}(u)$ can be derived as:

$$NE_{ARL}(u) \approx 1 + \frac{1}{\lambda+g} \sum_{j=1}^{2m+1} w_j \cdot E_{ARL}(x_j) \cdot f \left(\begin{array}{l} \dfrac{x_j - (1-\lambda)u + gF_{t-1}}{(\lambda+g)} \\ -(\theta_0 - \theta_1\varepsilon_{t-1} - \theta_2\varepsilon_{t-2} - \ldots - \theta_q\varepsilon_{t-q}) \\ -\left(\dfrac{a}{b}F_{t-1} + \dfrac{\frac{a}{b}(1-\frac{a}{b})}{2!}F_{t-2} + \dfrac{\frac{a}{b}(1-\frac{a}{b})(2-\frac{a}{b})}{3!}F_{t-3} + \ldots \right) \end{array} \right). \tag{15}$$

4- Research Methodology

In this research, the explicit formulas used to calculate the ARL on the modified EWMA control chart with either the IMA or FIMA model are obtained from Equations 7 and 14, respectively, while the ARLs for the NIE method are obtained from Equations 8 and 15, respectively. Meanwhile, $m = 500$. The bound control limits are studied on exponential distribution ε_t with interval $[0, \infty)$, where the lower control limit is 0 and the upper control limit is discovered for $ARL_0 = 370$; the latter is assigned by using exponential parameter β_0 for the in-control process and process mean $u = \beta_0$, $\varepsilon_{t-1}, \varepsilon_{t-2}, \ldots, \varepsilon_{t-q} = \beta_0$, $M_{t-1}, M_{t-2}, \ldots, M_{t-d} = \beta_0$, $F_{t-1}, F_{t-2}, F_{t-3}, \ldots = \beta_0$. After a change in the process mean, $\beta_1 = (1 + \delta)\beta_0$ becomes the exponential parameter for ARL_1 (the out-of-control process), where δ is the mean shift size. In the two models, β_1 is assigned with δ as 0.01, 0.02, 0.05, 0.10, 0.20, 0.50, 1.00, 1.50, or 2.00. The most efficient control chart achieves the lowest value of ARL_1.

The difference between the ARLs using the two techniques can be expressed as the absolute percentage relative change (APRC) [39] as follows:

$$\text{APRC}(\%) = \left| \frac{ARL_{Explicit} - ARL_{NIE}}{ARL_{Explicit}} \right| \times 100\%. \tag{16}$$

In addition, the relative mean index (RMI) [40] can also be used and is computed as:

$$\text{RMI} = \frac{1}{n} \sum_{i=1}^{n} \left[\frac{ARL_i(x) - ARL_i(min)}{ARL_i(min)} \right], \tag{17}$$

where $ARL_i(x)$ is the ARL of a control chart for order i and $ARL_i(min)$ is the minimum ARL of all of the control charts for order i. The control chart obtaining the smallest RMI is the best at detecting a shift in the process mean

The procedure shown in Figure 1 can be used to find solutions.

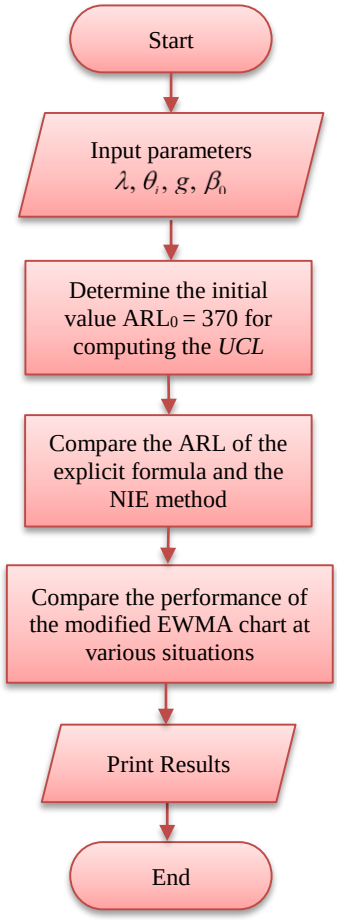

Figure 1. The diagram of the research process

5- Results

The solutions were tested both experimentally and with real data. Experimentally, the explicit formulas were used to compute the ARL on the modified EWMA control chart with either an IMA or FIMA model. The ARL results from the NIE method were used to confirm the results attained by using the explicit formulas. After that, the explicit formulas were used to compute the ARL under various sets of conditions. Afterward, the proposed control chart with an IMA or FIMA model was used to detect shifts in the mean of real datasets.

5-1- Experimental Study

In Table 1, the results for the explicit formula and the NIE methods for the ARL on the modified EWMA control chart with various IMA and FIMA models for $g = 1$ are reported for $\lambda = 0.05$, 0.10, or 0.20, various θ_i $(i = 1,2, \dots, q)$, and $ARL_0 = 370$. Since all of the APRC results for both methods are almost 0, their accuracies are almost identical. In addition, the explicit formulas were suddenly calculated. Meanwhile, the computation time for calculating the ARL by using the NIE method was 13-15 seconds with the IMA model and 32-40 seconds with the FIMA model. Therefore, the explicit formulas can be used to effectively and speedily detect a shift in the process mean on the modified EWMA control chart with either the IMA or FIMA model and exponential while noise.

Table 1. Compare the explicit formula and the NIE method with the initial ARL on various situations

Model	λ	θ_i (i =1, 2, …, q)	*UCL*	$ARL_{Explicit}$	ARL_{NIE}	APRC (%)
IMA (1,1)	0.05	0.1	0.408730497	370.0000489348190	370.0000489348737	1.45949×10^{-11}
		-0.1	0.333987011	370.0000881280786	370.0000881278731	5.53993×10^{-11}
	0.10	0.2	0.458429543	370.0001369929011	370.0001369929075	1.62849×10^{-12}
		-0.2	0.305078073	370.0000353347598	370.0000353346450	3.0803×10^{-11}
	0.20	0.5	0.64713764	370.0004513315197	370.0004513314839	9.72482×10^{-12}
		-0.5	0.229894994	370.0002675275411	370.0002675274683	1.97262×10^{-11}
IMA (2,2)	0.05	0.1, -0.3	0.301950105	370.0000281650370	370.0000281650863	1.3243×10^{-11}
		-0.1, -0.3	0.246857848	370.0002464590301	370.0002464591249	2.54105×10^{-11}
	0.10	0.2, 0.5	0.7668112894	370.0000077240967	370.0000077240489	1.29818×10^{-11}
		-0.2. 0.5	0.507821086	370.0001344921493	370.0001344921877	1.02625×10^{-11}
	0.20	0.5, -0.1	0.58240916	370.0002235870479	370.0002235870109	1.00014×10^{-11}
		-0.5. -0.1	0.20762702	370.0003278588000	370.0003278588756	2.02639×10^{-11}
FIMA (1/4,1)	0.05	0.1	0.648009914	370.0000207749287	370.0000207750297	2.73002×10^{-11}
		-0.1	0.528917341	370.0000422134455	370.0000422134522	1.88966×10^{-12}
	0.10	0.2	0.731614662	370.0000267918486	370.0000267918102	1.02625×10^{-11}
		-0.2	0.4847819	370.0002577550853	370.0002577551394	1.45949×10^{-11}
	0.20	0.5	1.054507842	370.0000603866825	370.0000603867113	7.85054×10^{-12}
		-0.5	0.366414073	370.0000362107346	370.0000362107134	5.66898×10^{-12}
FIMA (1/2,2)	0.05	0.1, -0.3	0.360682496	370.0000246901593	370.0000246902048	1.21522×10^{-11}
		-0.1, -0.3	0.294792246	370.0000942930957	370.0000942928763	5.9194×10^{-11}
	0.10	0.2, 0.5	0.9211324	370.0004824173434	370.0004824173442	2.76535×10^{-13}
		-0.2. 0.5	0.60853175	370.0002149586467	370.0002149586450	2.61172×10^{-13}
	0.20	0.5, -0.1	0.701536454	370.0000783111505	370.0000783111312	5.13127×10^{-12}
		-0.5. -0.1	0.24848627	370.0001283338770	370.0001283338820	1.35195×10^{-12}

The performance of the modified EWMA control chart with the IMA or FIMA model was studied with various values of g and λ (Tables 2 and 3, respectively). ARL_1 was calculated for each shift size δ. Note that for $g = 0$, the modified EWMA control chart is the same as the original EWMA scheme. The ARL results for the two models in one direction show that as the value of g was increased, the performance of the control chart improved. Moreover, for each value of g, the modified EWMA control chart was more effective than the original EWMA scheme for a small shift size. When λ was increased, the modified EWMA control chart produced a smaller ARL. The original EWMA scheme at $\lambda = 0.20$ provided a good performance when δ was small and, for intermediate-to-large shift sizes, it was more efficacious at $\lambda =$ 0.05.

Table 2. **Compare the modified EWMA chart on the IMA (2,1) model at various λ and g given $\theta = 0.05$ and l = 0**

λ	δ	$g = 0$ (EWMA)	$g = 0.2$	$g = 0.5$	$g = 1$	$g = 2$	$g = 5$
		$h = 1.471 \times 10^{-8}$	$h = 0.07209$	$h = 0.193428$	$h = 0.388592$	$h = 0.778267$	$h = 1.947165$
0.05	0.00	370	370	370	370	370	370
	0.01	297.967	291.663	141.174	81.541	57.930	46.253
	0.02	240.945	237.846	86.361	45.827	31.698	25.050
	0.05	130.617	146.166	38.882	19.841	13.739	10.943
	0.10	50.956	81.103	19.528	10.272	7.335	5.985
	0.20	10.365	36.035	9.300	5.358	4.067	3.461
	0.50	1.228	9.062	3.480	2.486	2.125	1.945
	1.00	1.005	3.142	1.912	1.628	1.512	1.451
	1.50	1.001	1.965	1.504	1.377	1.322	1.292
	2.00	1.000	1.555	1.333	1.264	1.233	1.215
		$h = 0.0006215$	$h = 0.080363$	$h = 0.197595$	$h = 0.393366$	$h = 0.786195$	$h = 1.96623$
0.10	0.00	370	370	370	370	370	370
	0.01	328.375	241.112	121.417	76.133	56.498	46.173
	0.02	292.121	176.189	72.032	42.493	30.868	25.004
	0.05	208.405	92.8609	31.801	18.363	13.383	10.924
	0.10	123.663	47.668	16.011	9.548	7.160	5.976
	0.20	49.713	20.906	7.776	5.031	3.986	3.457
	0.50	7.215	5.872	3.078	2.386	2.098	1.944
	1.00	1.747	2.428	1.786	1.591	1.501	1.451
	1.50	1.199	1.686	1.442	1.357	1.316	1.292
	2.00	1.080	1.412	1.296	1.251	1.228	1.215
		$h = 0.02526$	$h = 0.094336$	$h = 0.207968$	$h = 0.404355$	$h = 0.80287$	$h = 2.0053$
0.20	0.00	370	370	370	370	370	370
	0.01	287.262	154.532	93.577	67.375	53.938	46.037
	0.02	231.403	96.337	53.334	37.206	29.393	24.928
	0.05	138.240	43.632	23.077	16.052	12.752	10.892
	0.10	74.047	21.585	11.745	8.417	6.849	5.960
	0.20	31.189	9.914	5.920	4.519	3.841	3.450
	0.50	7.148	3.447	2.574	2.229	2.050	1.942
	1.00	2.438	1.822	1.622	1.532	1.482	1.450
	1.50	1.598	1.430	1.359	1.325	1.305	1.291
	2.00	1.326	1.273	1.245	1.230	1.220	1.214

Table 3. **Compare the modified EWMA chart on the FIMA (1/2,2) model at various λ and g given $\theta_1 = 0.05$, $\theta_2 = 0.10$, r = 0**

λ	δ	$g = 0$ (EWMA)	$g = 0.2$	$g = 0.5$	$g = 1$	$g = 2$	$g = 5$
		$s = 1.939 \times 10^{-8}$	$s = 0.09562$	$s = 0.255841$	$s = 0.513878$	$s = 1.029165$	$s = 2.574904$
0.05	0.00	370	370	370	370	370	370
	0.01	298.790	296.949	149.884	88.048	62.979	50.452
	0.02	242.256	245.398	93.131	49.999	34.716	27.477
	0.05	132.338	154.635	42.590	21.831	15.121	12.037
	0.10	52.228	87.724	21.585	11.347	8.081	6.577
	0.20	10.807	39.876	10.359	5.928	4.472	3.788
	0.50	1.250	10.291	3.879	2.728	2.309	2.100
	1.00	1.006	3.554	2.091	1.752	1.614	1.541
	1.50	1.001	2.174	1.615	1.460	1.393	1.357
	2.00	1.000	1.685	1.412	1.326	1.287	1.265

		s = 0.00082	s = 0.106567	s = 0.261963	s = 0.521639	s = 1.042775	s = 2.608302
0.10	0.00	370	370	370	370	370	370
	0.01	329.320	248.799	129.701	82.501	61.629	50.544
	0.02	293.781	184.902	78.057	46.506	33.920	27.531
	0.05	211.274	99.847	34.928	20.254	14.775	12.060
	0.10	126.905	52.143	17.718	10.565	7.909	6.590
	0.20	52.082	23.242	8.653	5.570	4.391	3.794
	0.50	7.827	6.626	3.416	2.616	2.282	2.103
	1.00	1.859	2.703	1.942	1.709	1.603	1.542
	1.50	1.236	1.834	1.539	1.437	1.387	1.358
	2.00	1.096	1.508	1.365	1.311	1.283	1.266
		s = 0.0335	s = 0.125369	s = 0.27688	s = 0.53902	s = 1.071231	s = 2.677395
0.20	0.00	370	370	370	370	370	370
	0.01	292.150	163.169	100.945	73.488	59.228	50.769
	0.02	238.110	103.364	58.228	40.957	32.513	27.660
	0.05	145.389	47.602	25.452	17.789	14.166	12.117
	0.10	79.401	23.783	13.017	9.344	7.607	6.619
	0.20	34.133	11.015	6.576	5.009	4.249	3.809
	0.50	8.001	3.832	2.835	2.440	2.234	2.109
	1.00	2.696	1.981	1.748	1.642	1.583	1.545
	1.50	1.721	1.523	1.440	1.399	1.375	1.360
	2.00	1.399	1.337	1.303	1.286	1.275	1.268

Tables 4 and 5 provide the RMI computations using the results from Tables 2 and 3, respectively. The RMI solutions in Table 4 when varying g while λ was fixed show that the modified EWMA control chart for the largest value of g attained the smallest RMI at each value of λ for both models, thereby signifying its excellent efficiency in both cases. In addition, for all values of g, the modified EWMA control chart performed better than the original EWMA scheme except for when g = 0.2 and λ = 0.05. In Table 5, when varying λ while g is fixed, the RMI for the original EWMA scheme was the lowest at λ = 0.05 and is thus the most suitable under these conditions, which is in accordance with previous research [41] for the EWMA control chart with an IMA (1,1) model. The modified EWMA control chart with g = 0.2, 0.5, 1, or 2 produced lower RMI values when λ was higher. However, the RMI for a high value of g (5) was similar for all values of λ. Therefore, the modified EWMA control chart can be recommended when g is large and with any value of λ. The RMI results are graphically displayed in Figure 2.

Table 4. Compare the RMI of two models at various g

Model	λ	g = 0 (EWMA)	g = 0.2	g = 0.5	g = 1	g = 2	g = 5
IMA (2,1)	0.05	3.451	5.814	1.457	0.595	0.296	0.153
	0.10	7.086	3.320	0.957	0.370	0.138	0.020
	0.20	4.837	1.391	0.550	0.240	0.088	0.000
FIMA (1/2,2)	0.05	3.153	5.815	1.512	0.638	0.331	0.183
	0.10	6.562	3.272	0.964	0.378	0.145	0.025
	0.20	4.623	1.364	0.545	0.239	0.088	0.000

Table 5. Compare the RMI of two models at various λ

Model	g	λ = 0.05	λ = 0.10	λ = 0.20
IMA (2,1)	0	0.008	1.212	0.969
	0.2	1.305	0.616	0.000
	0.5	0.375	0.210	0.000
	1	0.133	0.081	0.000
	2	0.044	0.028	0.000
	5	0.003	0.002	0.000

FIMA (1/2,2)	0	0.004	1.265	1.098
	0.2	1.292	0.614	0.000
	0.5	0.376	0.211	0.000
	1	0.130	0.080	0.000
	2	0.039	0.025	0.000
	5	0.000	0.001	0.004

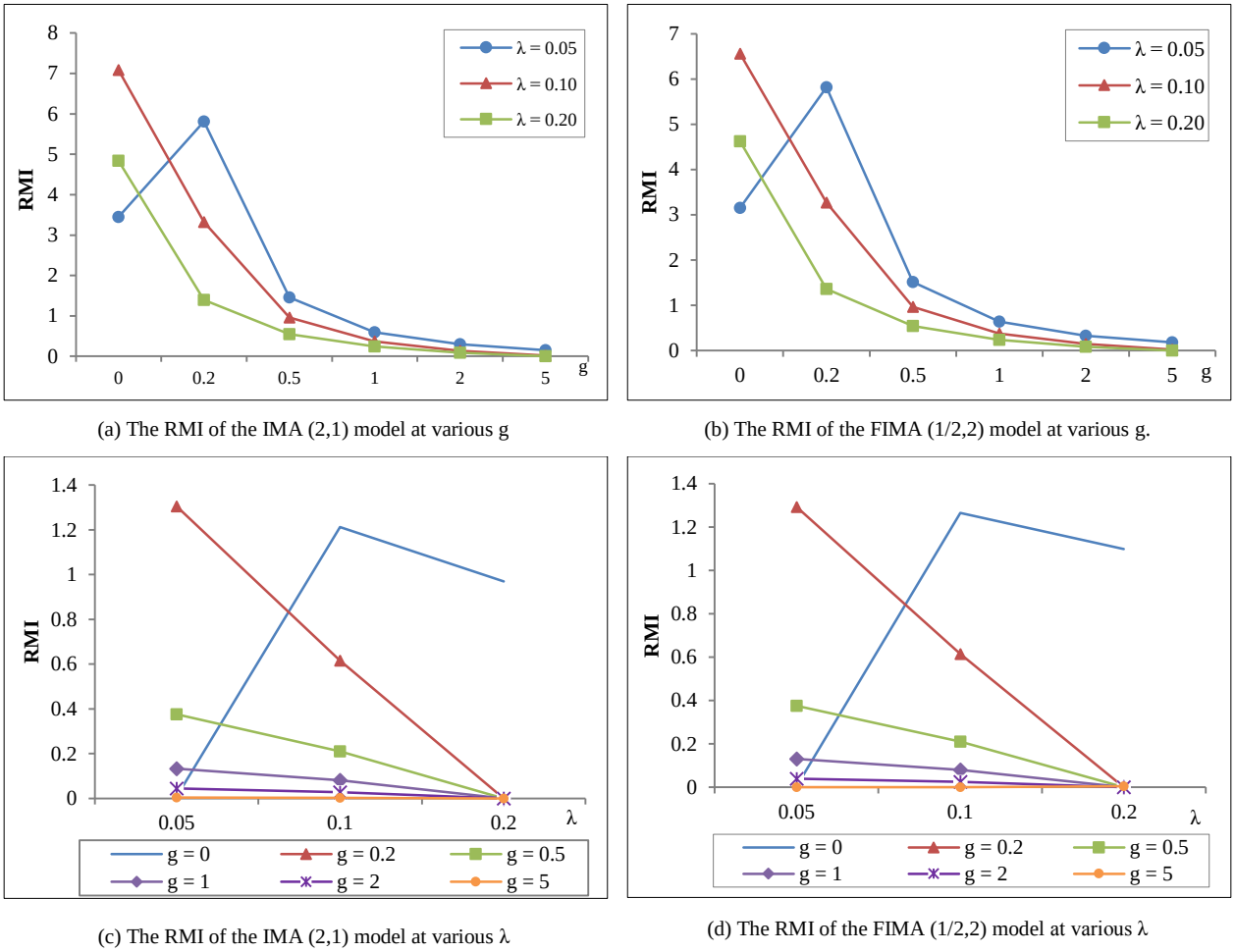

(a) The RMI of the IMA (2,1) model at various g

(b) The RMI of the FIMA (1/2,2) model at various g.

(c) The RMI of the IMA (2,1) model at various λ

(d) The RMI of the FIMA (1/2,2) model at various λ

Figure 2. The RMI of two models at various situations

5-2- Real Data Study

Oil and natural gas affect people in countless ways across the globe. They are used to fuel cars, heat homes, cook food, and generate electricity. Meanwhile, fuel consumption is steadily increasing while production is not. The price of oil and natural gas is influenced by the global stock market. For this research, the natural gas and WTI crude oil prices were used to analyze the IMA and FIMA models on the modified EWMA control chart: Dataset 1 is appropriate for the IMA model (the natural gas price from 1 March 2021 to 30 April 2021 [42]) while Dataset 2 is suitable for the FIMA model (the price of WTI crude oil from 1 Jan 2021 to 31 March 2021 [43]). For Dataset 1, the fitted equation for the IMA (2,1) model was $M_t = 0.0496 + \varepsilon_t - 0.925\varepsilon_{t-1} + 2M_{t-1} - M_{t-2}$ and for Dataset 2, the approximated FIMA (1/2,2) model was $F_t = 1.248 + \varepsilon_t + 0.304\varepsilon_{t-1} + 0.342\varepsilon_{t-2} + 0.5F_{t-1} + 0.125F_{t-2} + 0.0625F_{t-3} + \cdots$. After that, the residuals of two observations were tested by using a statistical hypothesis for an exponential distribution. The results show that Datasets 1 and 2 attained $\varepsilon_t \sim Exp(0.0496)$ and $\varepsilon_t \sim Exp(1.248)$, respectively.

The ARLs on the modified EWMA control charts for the natural gas price dataset using the IMA (2,1) model with various values of λ and g are given in Table 6 while those for the WTI crude oil price dataset using the FIMA (1/2,2) model are provided in Table 7. The results using the two datasets are in the same direction (Figure 3). For a small shift, the modified EWMA control chart for both models and datasets was more effective than the original EWMA scheme for all g except for λ = 0.05 and g = 0.2. In addition, the modified EWMA control chart preformed the best when g was large for all λ.

Table 6. Compare the modified EWMA charts on the IMA (2,1) model of the natural gas price at various λ and g

λ	δ	g = 0 (EWMA)	g = 0.2	g = 0.5	g = 1	g = 2	g = 5
		$h = 1.75 \times 10^{-9}$	h = 0.00881	h = 0.0233634	h = 0.0469033	h = 0.0939322	h = 0.235021
0.05	0.00	370	370	370	370	370	370
	0.01	300.506	309.799	173.854	107.448	78.571	63.683
	0.02	245.061	264.111	112.827	62.921	44.306	35.305
	0.05	136.112	176.928	53.913	28.156	19.588	15.605
	0.10	55.084	106.124	27.983	14.783	10.497	8.510
	0.20	11.834	51.057	13.676	7.748	5.779	4.848
	0.50	1.305	14.041	5.139	3.500	2.901	2.602
	1.00	1.008	4.849	2.663	2.151	1.942	1.832
	1.50	1.001	2.843	1.971	1.730	1.625	1.567
	2.00	1.000	2.105	1.666	1.530	1.467	1.432
		h = 0.0000743	h = 0.009817	h = 0.024122	h = 0.0480804	h = 0.0961863	h = 0.240722
0.10	0.00	370	370	370	370	370	370
	0.01	331.549	267.315	152.987	101.796	77.820	64.701
	0.02	297.568	207.091	95.890	59.138	43.842	35.915
	0.05	217.755	119.041	44.584	26.359	19.380	15.878
	0.10	134.321	65.005	23.067	13.868	10.393	8.651
	0.20	57.671	30.171	11.423	7.318	5.730	4.920
	0.50	9.380	8.935	4.490	3.361	2.885	2.630
	1.00	2.165	3.566	2.443	2.096	1.936	1.845
	1.50	1.339	2.308	1.857	1.699	1.622	1.576
	2.00	1.144	1.819	1.595	1.509	1.465	1.439
		h = 0.0030872	h = 0.0116452	h = 0.025889	h = 0.0506356	h = 0.1009743	h = 0.25302
0.20	0.00	370	370	370	370	370	370
	0.01	302.713	185.824	122.500	92.667	76.658	66.966
	0.02	253.436	122.827	73.196	53.164	43.127	37.274
	0.05	163.017	59.191	32.962	23.567	19.061	16.489
	0.10	93.348	30.352	17.086	12.451	10.235	8.967
	0.20	42.171	14.357	8.686	6.651	5.657	5.080
	0.50	10.457	5.025	3.681	3.143	2.863	2.693
	1.00	3.471	2.486	2.158	2.011	1.928	1.877
	1.50	2.099	1.824	1.707	1.651	1.618	1.597
	2.00	1.627	1.546	1.500	1.477	1.463	1.454

Table 7. Compare the modified EWMA charts on the FIMA (1/2,2) model of the price of WTI crude oil at various λ and g

λ	δ	g = 0 (EWMA)	g = 0.2	g = 0.5	g = 1	g = 2	g = 5
		$s = 3.973 \times 10^{-8}$	s = 0.19915	s = 0.5291	s = 1.0623	s = 2.12745	s = 5.32288
0.05	0.00	370	370	370	370	370	370
	0.01	300.198	307.344	168.950	103.296	75.165	60.754
	0.02	244.566	260.534	108.681	60.097	42.177	33.549
	0.05	135.451	172.549	51.470	26.756	18.588	14.801
	0.10	54.580	102.410	26.593	14.022	9.958	8.076
	0.20	11.650	48.748	12.956	7.347	5.489	4.612
	0.50	1.295	13.252	4.867	3.332	2.772	2.492
	1.00	1.008	4.573	2.540	2.064	1.871	1.768
	1.50	1.001	2.700	1.894	1.672	1.575	1.522
	2.00	1.000	2.015	1.611	1.486	1.428	1.396

		s = 0.001685	s = 0.22191	s = 0.545273	s = 1.0866	s = 2.1734	s = 5.43863
0.10	0.00	370	370	370	370	370	370
	0.01	331.063	264.050	148.219	97.649	74.235	61.521
	0.02	296.822	202.943	92.125	56.360	41.609	34.004
	0.05	216.560	115.237	42.496	24.998	18.335	15.003
	0.10	132.974	62.380	21.903	13.131	9.831	8.180
	0.20	56.650	28.732	10.821	6.930	5.429	4.665
	0.50	9.087	8.449	4.257	3.197	2.752	2.513
	1.00	2.105	3.382	2.334	2.0119	1.863	1.779
	1.50	1.319	2.207	1.788	1.642	1.570	1.528
	2.00	1.134	1.752	1.545	1.466	1.425	1.401
		s = 0.06977	s = 0.262723	s = 0.583194	s = 1.13944	s = 2.27043	s = 5.68584
0.20	0.00	370	370	370	370	370	370
	0.01	300.742	181.427	117.973	88.457	72.711	63.202
	0.02	250.601	118.924	69.977	50.428	40.678	35.003
	0.05	159.694	56.795	31.319	22.255	17.921	15.449
	0.10	90.657	28.976	16.192	11.746	9.623	8.410
	0.20	40.585	13.653	8.223	6.280	5.332	4.781
	0.50	9.959	4.772	3.496	2.986	2.720	2.559
	1.00	3.311	2.379	2.069	1.929	1.851	1.801
	1.50	2.020	1.759	1.649	1.595	1.564	1.543
	2.00	1.579	1.501	1.457	1.434	1.421	1.412

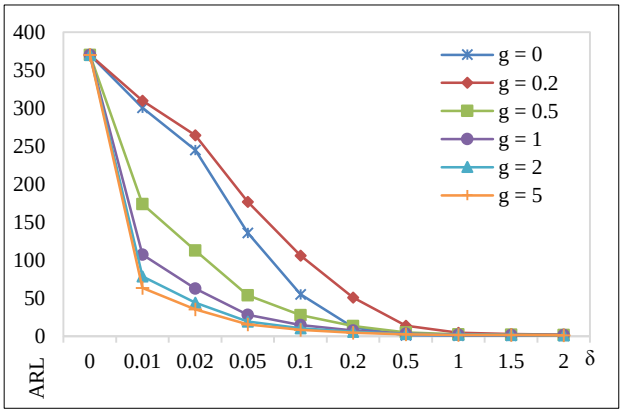

(a) The ARL for the natural gas price on the IMA(2,1) model at λ = 0.05.

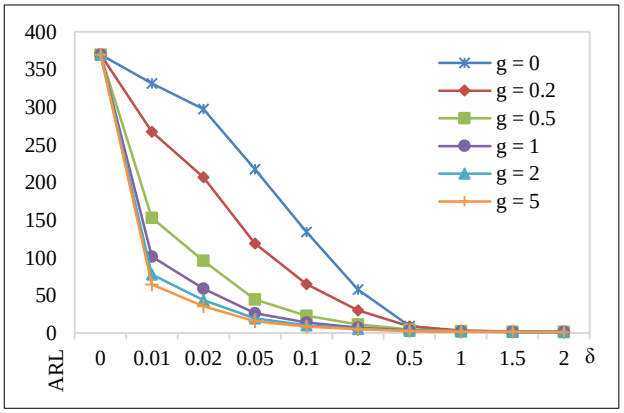

(b) The ARL for the natural gas price on the IMA(2,1) model at λ = 0.10

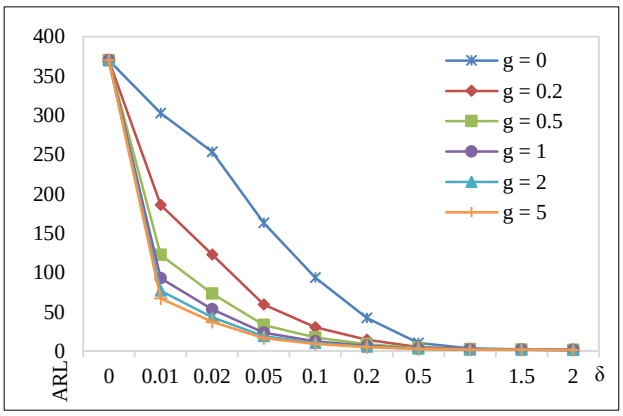

(c) The ARL for the natural gas price on the IMA(2,1) model at λ = 0.20

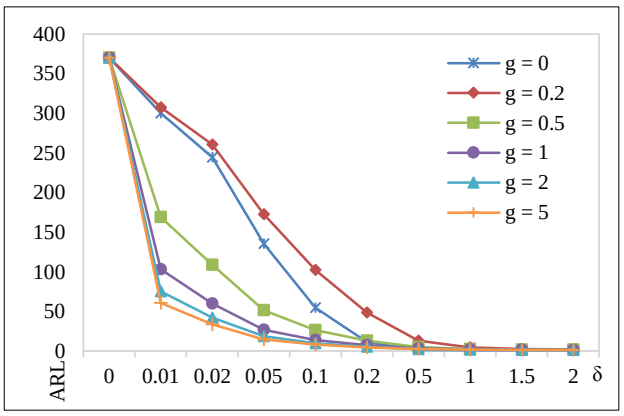

(d) The ARL for the price of WTI crude oil on the FIMA (1/2,2) model at λ = 0.05

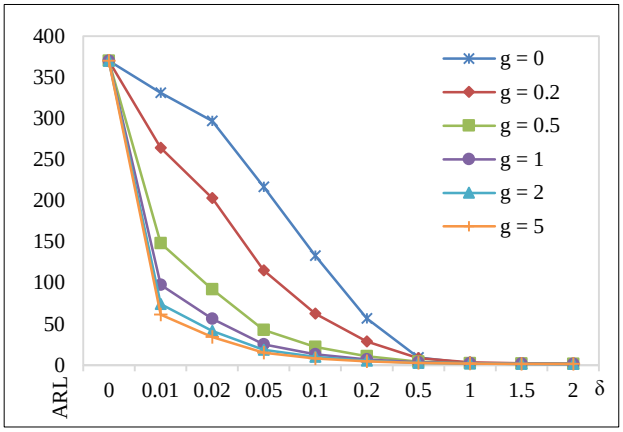

(e) The ARL for the price of WTI crude oil on the FIMA (1/2,2) model at λ = 0.10

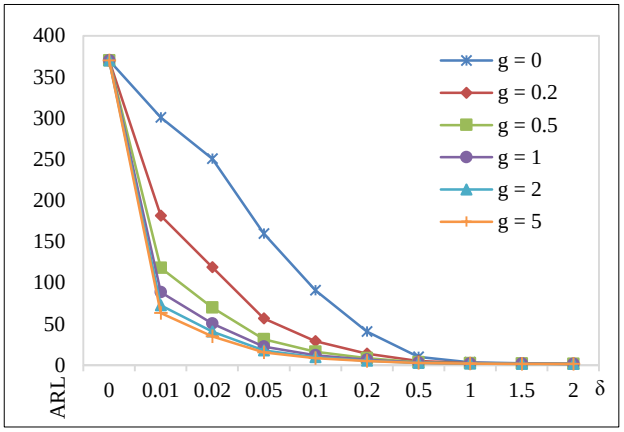

(f) The ARL for the price of WTI crude oil on the FIMA (1/2,2) model at λ = 0.20

Figure 3. The ARL of two datasets on the modified EWMA chart at various λ

The RMIs for the results in Tables 6 and 7 are reported in Tables 8 and 9, respectively, with a summary for both datasets being shown in Figure 4. In the first case, the modified EWMA control chart with the IMA or FIMA model for stable λ maintained their efficiency when g was enlarged. Moreover, the modified EWMA control chart could detect a shift in the process mean more quickly than the original EWMA scheme in most situations. Meanwhile, the modified EWMA control chart with the IMA or FIMA model produced better performances when λ was increased. However, for g = 5, the proposed chart and the original EWMA scheme attained the best efficacy at λ = 0.05. These results confirm those from the experimental study.

Table 8. Compare the RMI of two datasets at various g

Dataset	λ	g = 0 (EWMA)	g = 0.2	g = 0.5	g = 1	g = 2	g = 5
Natural gas IMA (2,1)	**0.05**	2.430	5.820	1.670	0.768	0.441	0.281
	0.10	5.211	3.069	0.964	0.397	0.165	0.043
	0.20	3.908	1.227	0.502	0.223	0.082	0.000
WTI Crude oil FIMA (1/2,2)	**0.05**	2.567	5.822	1.638	0.741	0.417	0.259
	0.10	5.474	3.121	0.967	0.394	0.161	0.039
	0.20	4.068	1.263	0.515	0.228	0.084	0.000

Table 9. Compare the RMI of two datasets at various λ

Dataset	g	λ = 0.05	λ = 0.10	λ = 0.20
Natural gas IMA (2,1)	0	0.000	1.405	1.468
	0.2	1.252	0.603	0.000
	0.5	0.370	0.208	0.000
	1	0.116	0.071	0.000
	2	0.015	0.009	0.000
	5	0.000	0.011	0.036
WTI Crude oil FIMA (1/2,2)	0	0.000	1.377	1.392
	0.2	1.260	0.606	0.000
	0.5	0.372	0.209	0.000
	1	0.120	0.073	0.000
	2	0.021	0.013	0.000
	5	0.000	0.009	0.028

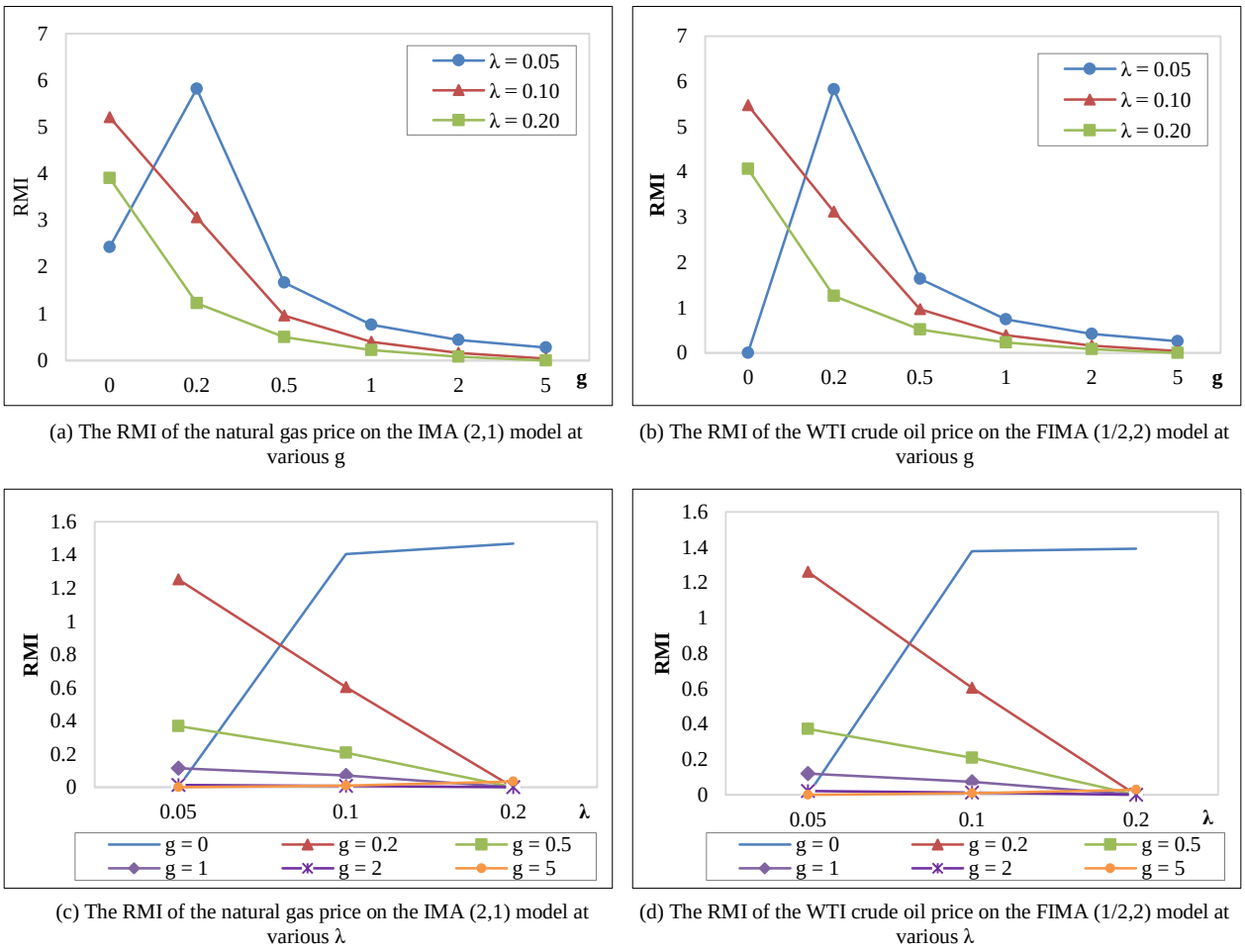

(a) The RMI of the natural gas price on the IMA (2,1) model at various g

(b) The RMI of the WTI crude oil price on the FIMA (1/2,2) model at various g

(c) The RMI of the natural gas price on the IMA (2,1) model at various λ

(d) The RMI of the WTI crude oil price on the FIMA (1/2,2) model at various λ

Figure 4. The RMI of two datasets at various situations

6- Conclusion

Herein, we present the modified EWMA control chart with IMA or FIMA models and exponential white noise and evaluate its performance by using the ARL. The equations for the IMA and FIMA models were rearranged by using a backward shift operator, after which they were merged with the modified EWMA statistic. The NIE method of the ARL for both models was derived under the control limits of the residuals to estimate the ARL, while explicit formulas for the two models were derived to solve the exact ARL. Afterward, the results obtained by using both techniques were compared to check their accuracy and computational speed. The original and modified EWMA control charts with the IMA or FIMA model were compared in terms of efficiency by using the results of ARL and RMI calculations. The modified EWMA control chart with either model was studied while varying the values of g and λ, and it was found that its efficacy improved as g was increased. Besides, increasing the value of λ enabled faster detection of process mean shifts on the modified EWMA control chart. Last, natural gas and WTI crude oil price datasets were used for the IMA and FIMA models, respectively. The results confirmed those obtained experimentally. These formulas could be applied to other real-life data following IMA and FIMA models, albeit the explicit formulas are limited to the residuals of an exponential distribution. Future studies will be conducted on explicit formulas for the ARL on modern control charts to improve their efficiency for parameter shift detection.

7- Declarations

7-1- Author Contributions

Conceptualization, P.P. and Y.A.; methodology, P.P.; software, P.P.; validation, P.P. and Y.A.; formal analysis, P.P.; investigation, Y.A.; resources, P.P.; data curation, Y.A.; writing—original draft preparation, P.P.; writing—review and editing, P.P.; visualization, P.P.; supervision, P.P.; project administration, P.P.; funding acquisition, P.P. All authors have read and agreed to the published version of the manuscript.

7-2- Data Availability Statement

These dataset to be oil and natural gas prices can be found here: *https://investing.com/commodities/natural-gas-historical-data* and *https://investing.com/commodities/crude-oil-historical-data*.

7-3- Funding and Acknowledgements

This research was supported by Rajamangala University of Technology Phra Nakhon (RMUTP).

7-4- Institutional Review Board Statement

Not applicable.

7-5- Informed Consent Statement

Not applicable.

7-6- Conflicts of Interest

The authors declare that there is no conflict of interest regarding the publication of this manuscript. In addition, the ethical issues, including plagiarism, informed consent, misconduct, data fabrication and/or falsification, double publication and/or submission, and redundancies have been completely observed by the authors.

8- References

[1] Shewhart, W. A. (1931). Economic control of quality of manufactured product. Macmillan And Co Ltd, London, United Kingdom.

[2] Page, E. S. (1954). Continuous Inspection Schemes. Biometrika, 41(1/2), 100. doi:10.2307/2333009.

[3] Roberts, S. W. (2000). Control chart tests based on geometric moving averages. Technometrics, 42(1), 97–101. doi:10.1080/00401706.2000.10485986.

[4] Patel, A. K., & Divecha, J. (2011). Modified exponentially weighted moving average (EWMA) control chart for an analytical process data. Journal of Chemical Engineering and Materials Science, 2(1), 12–20. doi:10.5897/JCEMS.9000014.

[5] Khan, N., Aslam, M., & Jun, C. H. (2017). Design of a Control Chart Using a Modified EWMA Statistic. Quality and Reliability Engineering International, 33(5), 1095–1104. doi:10.1002/qre.2102.

[6] Sunthornwat, R., & Areepong, Y. (2021). Reproduction number, discrete forecasting model, and chaos analytics for Coronavirus Disease 2019 outbreak in India, Bangladesh, and Myanmar. Biostatistics & Epidemiology, 6(1), 31–47. doi:10.1080/24709360.2021.1960122.

[7] Tatarkanov, A. A., Alexandrov, I. A., Chervjakov, L. M., & Karlova, T. V. (2022). A Fuzzy Approach to the Synthesis of Cognitive Maps for Modeling Decision Making in Complex Systems. Emerging Science Journal, 6(2), 368-381. doi: 10.28991/ESJ-2022-06-02-012.

[8] Karevan, Z., & Suykens, J. A. K. (2020). Transductive LSTM for time-series prediction: An application to weather forecasting. Neural Networks, 125, 1–9. doi:10.1016/j.neunet.2019.12.030.

[9] Jiang, Z., Tahmasebi, P., & Mao, Z. (2021). Deep residual U-net convolution neural networks with autoregressive strategy for fluid flow predictions in large-scale geosystems. Advances in Water Resources, 150, 103878. doi:10.1016/j.advwatres.2021.103878.

[10] Khozani, Z. S., Banadkooki, F. B., Ehteram, M., Ahmed, A. N., & El-Shafie, A. (2022). Combining autoregressive integrated moving average with Long Short-Term Memory neural network and optimisation algorithms for predicting ground water level. Journal of Cleaner Production, 348, 131224. doi: 10.1016/j.jclepro.2022.131224.

[11] Yang, Y., Yang, L., & Yao, G. (2021). Post-processing of high formwork monitoring data based on the back propagation neural networks model and the autoregressive—moving-average model. Symmetry, 13(8), 1543. doi:10.3390/sym13081543.

[12] Schaffer, A. L., Dobbins, T. A., & Pearson, S. A. (2021). Interrupted time series analysis using autoregressive integrated moving average (ARIMA) models: a guide for evaluating large-scale health interventions. BMC Medical Research Methodology, 21(1). doi:10.1186/s12874-021-01235-8.

[13] Yuan, X., Tan, Q., Lei, X., Yuan, Y., & Wu, X. (2017). Wind power prediction using hybrid autoregressive fractionally integrated moving average and least square support vector machine. Energy, 129, 122–137. doi:10.1016/j.energy.2017.04.094.

[14] Franses, P. H. (2020). IMA(1,1) as a new benchmark for forecast evaluation. Applied Economics Letters, 27(17), 1419–1423. doi:10.1080/13504851.2019.1686115.

[15] Burnecki, K., Kepten, E., Garini, Y., Sikora, G., & Weron, A. (2015). Estimating the anomalous diffusion exponent for single particle tracking data with measurement errors-An alternative approach. Scientific Reports, 5, 11306. doi:10.1038/srep11306.

[16] Kacker, R., & Zhang, N. F. (2002). Online control using integrated moving average model for manufacturing errors. International Journal of Production Research, 40(16), 4131–4146. doi:10.1080/00207540210155800.

[17] Luceno, A. (1995). Choosing the EWMA parameter in engineering process control. Journal of Quality Technology, 27(2), 162–168. doi:10.1080/00224065.1995.11979579.

[18] Lee, S., Ahn, W. Y., & Kang, H. C. (2010). A Study on Forecasting Traffic Congestion Using IMA (Integrated Moving Average) of Speed Sequence Array. KSCE Journal of Civil and Environmental Engineering Research, 30(2D), 113-118. (In Korean).

[19] Burnecki, K., Sikora, G., Weron, A., Tamkun, M. M., & Krapf, D. (2019). Identifying diffusive motions in single-particle trajectories on the plasma membrane via fractional time-series models. Physical Review E, 99(1), 12101. doi:10.1103/PhysRevE.99.012101.

[20] Moffat, I. U., & Akpan, E. A. (2019). White Noise Analysis: A Measure of Time Series Model Adequacy. Applied Mathematics, 10(11), 989–1003. doi:10.4236/am.2019.1011069.

[21] Knoth, S. (2021). Steady-state average run length(s): Methodology, formulas, and numerics. Sequential Analysis, 40(3), 405–426. doi:10.1080/07474946.2021.1940501.

[22] Khan, M., Aslam, M., Anwar, S. M., & Zaman, B. (2022). A robust hybrid exponentially weighted moving average chart for monitoring time between events. Quality and Reliability Engineering International, 38(2), 895–923. doi:10.1002/qre.3021.

[23] Zaman, B., Lee, M. H., Riaz, M., & Abujiya, M. R. (2020). An improved process monitoring by mixed multivariate memory control charts: An application in wind turbine field. Computers and Industrial Engineering, 142, 106343. doi:10.1016/j.cie.2020.106343.

[24] Petcharat, K. (2022). The Effectiveness of CUSUM Control Chart for Trend Stationary Seasonal Autocorrelated Data. Thailand Statistician, 20(2), 475–488.

[25] Peerajit, W. (2022). Cumulative Sum Control Chart Applied to Monitor Shifts in the Mean of a Long-memory ARFIMAX(p, d*, q, r) Process with Exponential White Noise. Thailand Statistician, 20(1), 144–161.

[26] Petcharat, K., Sukparungsee, S., & Areepong, Y. (2015). Exact solution of the average run length for the cumulative sum chart for a moving average process of order q. ScienceAsia, 41(2), 141–147. doi:10.2306/scienceasia1513-1874.2015.41.141.

[27] Sunthornwat, R., Areepong, Y., & Sukparungsee, S. (2017). Average run length of the long-memory autoregressive fractionally integrated moving average process of the exponential weighted moving average control chart. Cogent Mathematics, 4(1), 1358536. doi:10.1080/23311835.2017.1358536.

[28] Sunthornwat, R., & Areepong, Y. (2020). Average run length on CUSUM control chart for seasonal and non-seasonal moving average processes with exogenous variables. Symmetry, 12(1), 173. doi:10.3390/SYM12010173.

[29] Phanthuna, P., Areepong, Y., & Sukparungsee, S. (2021). Exact run length evaluation on a two-sided modified exponentially weighted moving average chart for monitoring process mean. CMES - Computer Modeling in Engineering and Sciences, 127(1), 23–41. doi:10.32604/cmes.2021.013810.

[30] Phanthuna, P., Areepong, Y., & Sukparungsee, S. (2021). Run length distribution for a modified EWMA scheme fitted with a stationary AR(p) model. Communications in Statistics - Simulation and Computation, 1–20. doi:10.1080/03610918.2021.1958847.

[31] Supharakonsakun, Y., Areepong, Y., & Sukparungsee, S. (2020). Monitoring the Process Mean of a Modified EWMA Chart for Arma(1,1) Process and Its Application. Suranaree Journal of Science and Technology, 27(4), 1–11.

[32] Supharakonsakun, Y., Areepong, Y., & Sukparungsee, S. (2020). The performance of a modified EWMA control chart for monitoring autocorrelated PM2.5 and carbon monoxide air pollution data. PeerJ, 8, e10467. doi:10.7717/peerj.10467.

[33] Supharakonsakun, Y. (2021). Comparing the effectiveness of statistical control charts for monitoring a change in process mean. Engineering Letters, 29(3), 1108–1114.

[34] Spivey, M. Z. (2019). The art of proving binomial identities (1st Ed.). CRC Press, boca raton, United States. doi:10.1201/9781351215824.

[35] Avazzadeh, Z., Heydari, M., & Loghmani, G. B. (2011). Numerical solution of Fredholm integral equations of the second kind by using integral mean value theorem. Applied Mathematical Modelling, 35(5), 2374–2383. doi:10.1016/j.apm.2010.11.056.

[36] Shukla, S., Balasubramanian, S., & Pavlović, M. (2016). A Generalized Banach Fixed Point Theorem. Bulletin of the Malaysian Mathematical Sciences Society, 39(4), 1529–1539. doi:10.1007/s40840-015-0255-5.

[37] Karoon, K., Areepong, Y., & Sukparungsee, S. (2021). Numerical Integral Equation Methods of Average Run Length on Extended EWMA Control Chart for Autoregressive Process. Proceedings of the World Congress on Engineering (WCE 2021), July 7-9, 2021, London, United Kingdom.

[38] Liu, C. (2010). The essence of the generalized Newton binomial theorem. Communications in Nonlinear Science and Numerical Simulation, 15(10), 2766–2768. doi:10.1016/j.cnsns.2009.11.004.

[39] Areepong, Y., & Peerajit, W. (2022). Integral equation solutions for the average run length for monitoring shifts in the mean of a generalized seasonal ARFIMAX(P, D, Q, r)s process running on a CUSUM control chart. PLOS ONE, 17(2), e0264283. doi:10.1371/journal.pone.0264283.

[40] Phanthuna, P., & Areepong, Y. (2021). Analytical solutions of ARL for SAR(P)l model on a modified EWMA chart. Mathematics and Statistics, 9(5), 685–696. doi:10.13189/ms.2021.090508.

[41] Suriyakat, W. (2020). On sensitivity of control chart for monitoring serially correlated data. Interdisciplinary Research Review, 15(3), 44-47.

[42] Fusion Media (2022). Natural gas futures historical data. Available online: https://www.investing.com/commodities/natural-gas-historical-data (accessed on June 2022).

[43] Fusion Media (2022). Crude oil WTI Futures historical prices 2018-2021. Available online: https://www.investing.com/commodities/crude-oil-historical-data (accessed on May 2022).